Quantification of Temporal Decorrelation Effects at L-Band for Polarimetric SAR Interferometry Applications

Seung-Kuk Lee, Florian Kugler, Konstantinos P. Papathanassiou, *Senior Member, IEEE*, and Irena Hajnsek, *Member, IEEE*

***Abstract*—Temporal decorrelation is the most critical issue for the successful inversion of polarimetric SAR interferometry (Pol-InSAR) data acquired in an interferometric repeat-pass mode, typical for satellite or lower frequency airborne SAR systems. This paper provides a quantitative estimation of temporal decorrelation effects at L-band for a wide range of temporal baselines based on a unique set of multibaseline Pol-InSAR data. A new methodology that allows to quantify individual temporal decorrelation components has been developed and applied. Temporal decorrelation coefficients are estimated for temporal baselines ranging from 10 min to 54 days and converted to height inversion errors caused by them. The temporal decorrelations of γ_{TV} (volume temporal decorrelation) and γ_{TG} (ground temporal decorrelation) depend not only on the wind-induced movement but also strongly on the rain-induced dielectric changes in volume and on the ground at temporal baseline on the order of day or longer. At temporal baselines on the order of minutes, the wind speed is a critical parameter and the speed of 2 m/s already hampers the application of Pol-InSAR forest parameter inversion. The approach is supported and validated by using L-band E-SAR repeat-pass data acquired in the frame of three dedicated campaigns, BioSAR 2007, TempoSAR 2008, and TempoSAR 2009.**

***Index Terms*—Height inversion, polarimetric synthetic aperture radar interferometry (Pol-InSAR), temporal baseline, temporal decorrelation.**

I. Introduction

POLARIMETRIC synthetic aperture radar interferometry (Pol-InSAR) has been developed to a powerful technique for quantitative forest applications. The Pol-InSAR technique is based on the combination of two important SAR measurements: interferometry and polarimetry. Interferometric SAR (InSAR) is sensitive to the vertical structure of volume scatterers as forest and allows to estimate accurately the vertical position of the scattering center. Polarimetric SAR (PolSAR) is able to identify shape, orientation and dielectric properties of scatters allowing the understanding of scattering mechanisms. In [1], the coherent combination of the two techniques was first introduced to provide the separation and the identification of different scattering contributions within the resolution cell. In the last decade, a variety of quantitative models for the estimation of forest parameters from Pol-InSAR data, as the Random Volume over Ground (RVoG) model, have been developed and successfully validated over a variety of forest test sites [2]–[5].

The key observable used in Pol-InSAR application is the complex interferometric coherence estimated at different polarizations. The interferometric coherence depends on instrument and acquisition parameters as well as on dielectric and structural parameters of the scatterer. The total interferometric coherence can be decomposed into several decorrelation processes [6], [7]: System induced noise decorrelation, temporal decorrelation, volume decorrelation and so on. To invert forest parameters by means of Pol-InSAR technique, volume decorrelation $\tilde{\gamma}_V$ must be separated from other decorrelation contributions because the RVoG model only considers the volume decorrelation contribution of the interferometric coherence ignoring other decorrelation contributions. Uncompensated nonvolumetric decorrelation contributions lower the interferometric coherence, and increase the variation of the interferometric phase leading to a biased and less accurate parameter estimation performance. In repeat-pass air- or spaceborne InSAR configurations, the most critical nonvolumetric decorrelation contribution is the temporal decorrelation caused by the change of the geometric and/or dielectric properties of the scatterers within the scene occurring in the time between the two acquisitions.

In previous studies, temporal decorrelation was modeled assuming only changes in the position of the scatterers. If the motion of the scatterers is characterized by a Gaussian-statistic an exponential temporal decorrelation model is derived [7]. This model was first validated using L-band SEASAT data. The exponential model was extended by a Brownian motion [8]. The Brownian motion implies an exponential decay of the temporal decorrelation with time. However, the temporal decorrelation in forest at small temporal baselines (i.e., shorter than an hour) is mainly caused by wind-induced motion making the Brownian motion inadequate to model temporal decorrelation at these temporal baseline scales [16]. More recently, a physical model of temporal decorrelation was proposed assuming a variable Gaussian motion along the vertical direction of forests [15]. This model was validated at L-band using zero spatial baseline and 40-min temporal baseline data acquired by the JPL's UAVSAR system.

However, all temporal decorrelation models proposed the assumption that the dielectric properties of the scatterers remain

Manuscript received October 07, 2012; revised December 07, 2012; accepted February 07, 2013. Date of publication April 26, 2013; date of current version June 17, 2013.

S.-K. Lee and I. Hajnsek are with the Institute of Environmental Engineering, ETH Zurich, CH-8093 Zurich, Switzerland and with Microwaves and Radar Institute, German Aerospace Center, 82234 Wessling, Germany (e-mail: leeseu@ethz.ch; seungkuk.lee@dlr.de; ihajnsek@ethz.ch; irena.hajnsek@dlr.de).

F. Kugler and K. P. Papathanassiou are with Microwaves and Radar Institute, German Aerospace Center, 82234 Wessling, Germany (e-mail: florian.kugler@dlr.de; kostas.papathanassiou@dlr.de).

Color versions of one or more of the figures in this paper are available online at http://ieeexplore.ieee.org.

Digital Object Identifier 10.1109/JSTARS.2013.2253448

unchanged between the two acquisitions. At long temporal baselines (i.e., longer than a day), temporal decorrelation may be also caused by the change of dielectric properties due to environmental and weather effects.

There are different approaches to assess the impact of temporal decorrelation on the Pol-InSAR forest height inversion. The RVoG with Volume Temporal Decorrelation (RVoG + VTD) model was introduced in [9], [4] incorporating a temporal decorrelation component into the two-layer (volume/ground) scattering model. The inversion results in the presence of temporal decorrelation (2 day) demonstrated that forest height inversion without accounting or compensating for temporal decorrelation leads to significantly overestimated heights [9]. In [5], the quantification of temporal decorrelation in L- and P-band repeat-pass interferograms was discussed in the context of the INDREX-II data sets acquired with about 40-min temporal baseline assuming that the scattering properties of the ground do not change in that time. For the special case of a zero (spatial) baseline interferogram, temporal decorrelations at L- and P-band are separated from volume decorrelation. The obtained results in homogenous forest area indicated, as expected, a lower temporal stability for higher frequencies, and that patterns of wind-induced temporal decorrelation do not correlate with forest structure and may change from interferogram to interferogram even if they are acquired with the same temporal baseline (i.e., 40 min). While this method can provide an estimation of temporal decorrelation, the impact of temporal decorrelation on Pol-InSAR forest height inversion cannot be directly addressed due to the absence of volume decorrelation $\tilde{\gamma}_V$.

This paper focuses on a quantitative analysis of temporal decorrelation on Pol-InSAR inversion performance at L-band as a function of temporal baseline based on multitemporal and multispatial airborne experimental data acquired in the frame of three dedicated airborne SAR experiments. Different temporal decorrelation coefficients for volume and the ground scattering are incorporated into RVoG model. Both deteriorate the interferometric coherence on different time scales. By using the experimental data, the decorrelation contributions are separated from each other even for nonzero spatial baselines. The behavior of both temporal decorrelations and their impact on forest height inversion performance is analyzed and discussed as a function of time.

To investigate the analysis of temporal decorrelation in time, three dedicated airborne SAR campaigns (BioSAR 2007, TempoSAR 2008 and TempoSAR 2009) carried out over boreal and temperate forest sites by DLR's airborne Experimental SAR system, E-SAR [11] are investigated. During the campaigns, DLR's E-SAR system collected fully polarimetric and repeat-pass interferometric SAR data on a variety of temporal and spatial baselines. Section II of this paper will introduce the RVoG model with two temporal decorrelation parameters and show simulation results of their impact on forest height inversion performance. The airborne campaigns are described including test sites and Pol-InSAR data sets in Section III. In Section IV, the impact of temporal decorrelation on Pol-InSAR inversion performance is discussed and validated by real airborne experimental data at temporal baselines on the order of 10 min to 54 d. Finally, the obtained results are reviewed and discussed in Section VI.

II. Temporal Decorrelation in Pol-InSAR

Quantitative estimation of forest parameters has been successfully performed by using a two-layer model, the so-called Random Volume over Ground (RVoG) model [3]–[5]. The RVoG model consists of a volume layer containing randomly oriented scatterers and an impenetrable ground layer. The interferometric coherence is directly linked to the vertical distribution of scatterers through a (normalized) Fourier transformation relationship [1]–[3]. Accordingly, the ground layer is modeled by the Dirac delta function located at interface between the two media. After range filtering [6] and compensation of system induced noise decorrelation [10], the interferometric coherence at the ground layer becomes unity and the phase center in the vertical direction (z) is located on the ground ϕ_0:

$$\tilde{\gamma} = e^{i\kappa_z z_0} \frac{\int_0^{h_v} \delta(z') e^{i\kappa_z z'} dz'}{\int_0^{h_v} \delta(z') dz'} = e^{i\phi_0} \tag{1}$$

κ_z is the effective vertical (interferometric) wavenumber and the phase $\phi_0 = \kappa_z z_0$ is related to the ground topography. Differently than the surface scattering, the volume layer is characterized by an extended distribution of scatterers. In the simplest case, the vertical distribution of scatterers in volume is assumed to be an exponential function defined by a mean extinction coefficient expressing both scattering and absorption losses. Accordingly the interferometric coherence for the volume is given as [3]–[5]

$$\tilde{\gamma}_V = \frac{\int_0^{h_v} F(z') e^{i\kappa_z z'} dz'}{\int_0^{h_v} F(z') dz'} = \frac{\int_0^{h_v} e^{\frac{2\sigma z'}{\cos\theta_0}} e^{i\kappa_z z'} dz'}{\int_0^{h_v} e^{\frac{2\sigma z'}{\cos\theta_0}} dz'}. \tag{2}$$

Combining surface and volume scatterings, the coherence for the RVoG model is obtained as [4], [5]

$$\begin{aligned} \tilde{\gamma}(\vec{w}) &= e^{i\phi_0} \frac{\tilde{\gamma}_V + m(\vec{w})}{1 + m(\vec{w})} \\ &= e^{i\phi_0} \left(\tilde{\gamma}_V + \frac{m(\vec{w})}{1 + m(\vec{w})} (1 - \tilde{\gamma}_V) \right) \end{aligned} \tag{3}$$

where m is the effective surface-to-volume scattering amplitude ratio accounting for the attenuation through the volume. The coherences $\tilde{\gamma}(\vec{w})$ at different polarizations $\vec{w}$ vary only due to the variation of the ground-to-volume amplitude ratio with polarization. In Fig. 1, they are plotted on the complex plane. These loci lie on a straight line. Neglecting temporal decorrelation and assuming a sufficient calibration/compensation of system- and geometry-induced decorrelation contributions, (3) can be inverted using a quad-polarization single-baseline acquisition. In the conventional monostatic case, three interferometric coherences formed by using the three independent polarizations are available to estimate five unknown parameters $(h_v, \sigma, \phi_0, m_1, m_2)$ assuming that one polarization has no ground response $(m_3 = 0)$ [2], [4], [5].

However, in repeat-pass airborne/satellite InSAR (or Pol-InSAR) system, temporal decorrelation introduced by dynamic changes within the scene cannot be neglected. Temporal decorrelation affects in general both the volume component that represents the vegetation layer and the underlying ground layer, but the decorrelation processes occur differently in the two layers. Temporal decorrelation on the ground layer can arise from surface changes between the two acquisitions. The

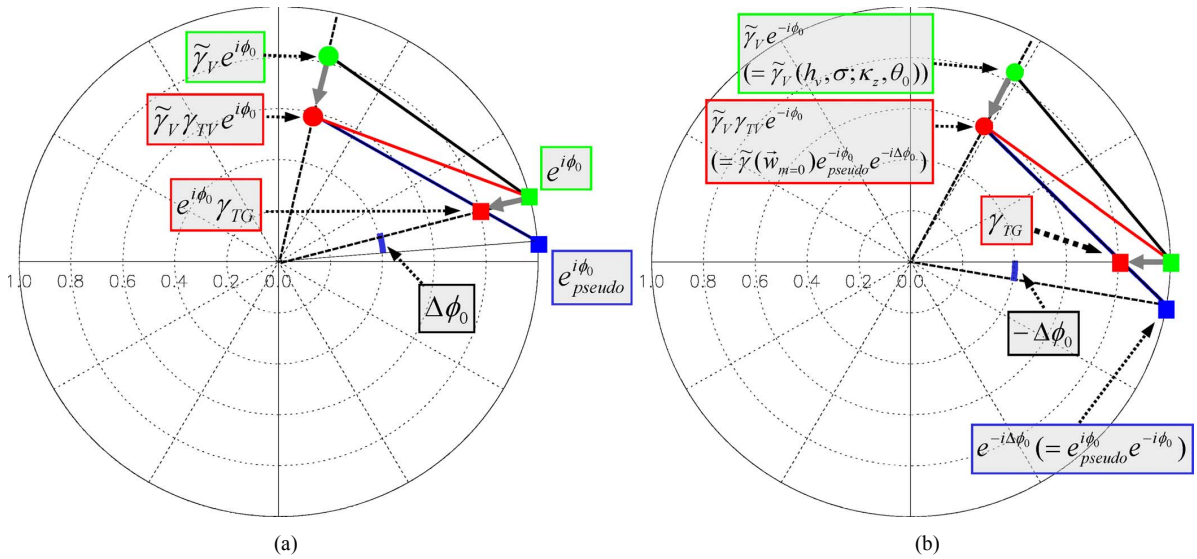

Fig. 1. (a) Coherence loci for the RVoG model with temporal decorrelations of γ_{TV} and γ_{TG}. (b) Coherence loci rotated by ground phase $e^{-i\phi_0}(=e^{-i\phi_0}_{pseudo}e^{-i\Delta\phi_0})$; Temporal decorrelation on the ground layer γ_{TG} is located on x-axis.

ground point that represents the interferometric coherence on the ground can be modified as

$$\tilde{\gamma}(\vec{w}_{m=\infty}) = \gamma_{\mathrm{TG}} e^{i\kappa_z z_0} \frac{\int_0^{h_v} \delta(z') e^{i\kappa_z z'}\, dz'}{\int_0^{h_v} \delta(z')\, dz'} = \gamma_{\mathrm{TG}} e^{i\phi_0} \quad (4)$$

where $\delta(\cdot)$ is a Dirac delta function and γ_{TG} represents the *scalar* correlation coefficient describing temporal decorrelation of the underlying surface scatterers [9]. In a unit circle, γ_{TG} results in a shift of the ground point $e^{i\phi_0}$ radially towards the origin as shown in Fig. 1, but the phase center remains unchanged. On the other hand, temporal decorrelation in volume is more complex and critical due to its susceptibility to wind which is nonstationary neither temporally nor spatially even on very short time- and small spatial-scales. Assuming that temporal decorrelation varies along the vertical structure function, volume decorrelation in (2) can be modified by a temporal decorrelation structure function $F_t(z)$ given as [15]

$$\tilde{\gamma}(\vec{w}_{m=0}) = \frac{\int_0^{h_v} F_t(z') F(z') e^{i\kappa_z z'}\, dz'}{\int_0^{h_v} F(z')\, dz'} = \tilde{\gamma}_{\mathrm{TV}} \tilde{\gamma}_V. \quad (5)$$

$\tilde{\gamma}_{\mathrm{TV}}$ denotes the *complex* correlation coefficient describing the temporal decorrelation of the volume layer. In this case, temporal decorrelation reduces the amplitude of volume decorrelation and changes the effective phase center depending on the temporal structure function. In case of a constant temporal decorrelation function, temporal decorrelation in volume becomes a *scalar* value γ_{TV} (i.e., no bias of phase).

Both temporal decorrelation effects can be incorporated in the two-layer scattering model. The equation of RVoG model [see (3)] with two temporal decorrelations can be described as [9], [15]

$$\tilde{\gamma}(\vec{w}) = e^{i\phi_0} \frac{\tilde{\gamma}_{\mathrm{TV}} \tilde{\gamma}_V + \gamma_{\mathrm{TG}} m(\vec{w})}{1 + m(\vec{w})}. \quad (6)$$

Both $\tilde{\gamma}_{\mathrm{TV}}$ and γ_{TG} are functions of the temporal baseline; however the decorrelation processes in the volume layer occur at different—in general much smaller—time scales than the decorrelation of the surface layer. Moreover, both temporal decorrelation coefficients may be polarization dependent: For example, changes in the dielectric properties of the canopy layer (due to changes in moisture content) or even more changes in its structural characteristics (caused by the annual phenological cycle or fire events) lead to different changes at different polarizations in the volume scatterers. Furthermore, a change in the dielectric properties of the ground—as for example due to a change in soil moisture—effects the scattering at each polarization differently and leads to a polarization dependent temporal decorrelation of the ground.

Using a quad-polarization single baseline acquisition (three complex coherences), (6) cannot be inverted even in a multibaseline configuration due to the two additional unknown parameters $(\tilde{\gamma}_{\mathrm{TV}}, \gamma_{\mathrm{TG}})$ introduced by any (temporal) baseline. However, even if the general temporal decorrelation scenario of (6) is underdetermined, special temporal decorrelation scenarios allowing simple assumptions may be accounted for in the context of multibaseline Pol-InSAR acquisitions, as it will be discussed in the next section.

A. Wind Induced Temporal Decorrelation

When the temporal baseline is sufficiently short (i.e., smaller than 1 h), it is realistic to assume that the ground remains stable (i.e., $\gamma_{\mathrm{TG}} = 1$), and that the dielectric and statistical properties of the volume do not change. Thus, the most common temporal decorrelation in forest is due to wind-induced movement of the scatterers within the volume layer. In this case, the RVoG model with temporal decorrelation contributions mentioned in (6) can be simplified as [4], [5], [9]

$$\begin{aligned}\tilde{\gamma}(\vec{w}) &= e^{i\phi_0} \frac{\gamma_{\mathrm{TV}} \tilde{\gamma}_V + m(\vec{w})}{1 + m(\vec{w})} \\ &= e^{i\phi_0} \left(\gamma_{\mathrm{TV}} \tilde{\gamma}_V + \frac{m(\vec{w})}{1 + m(\vec{w})} (1 - \gamma_{\mathrm{TV}} \tilde{\gamma}_V) \right). \quad (7)\end{aligned}$$

The Pol-InSAR coherence loci contaminated by γ_{TV} still lie on a straight line segment in the complex plane. The ground

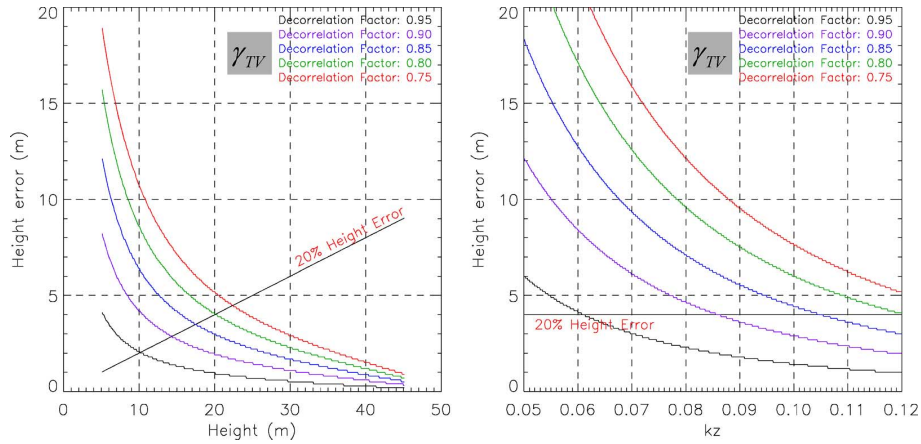

Fig. 2. (a) Height bias (overestimation) induced by different levels of temporal decorrelation as a function of forest heights assuming a constant vertical wavenumber of $\kappa_z = 0.12$ rad/m. (b) Height bias induced by different levels of temporal decorrelation as a function of vertical wavenumber κ_z, assuming a constant forest height of 20 m.

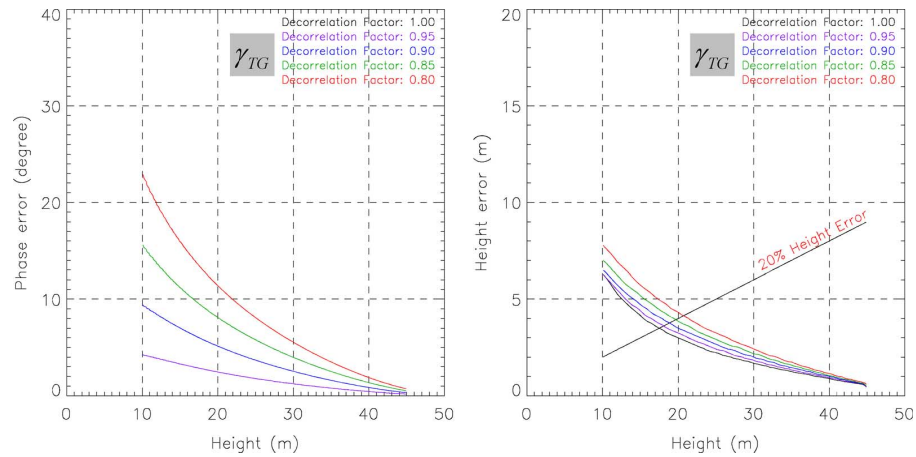

Fig. 3. Biases caused by γ_{TG}. Ground phase bias $\Delta\phi_0$ (a) and height bias Δh (b) induced by different levels of temporal decorrelation γ_{TG} as a function of forest height assuming a vertical wavenumber of $\kappa_z = 0.12$ rad/m and temporal decorrelation of $\gamma_{\mathrm{TV}} = 0.85$.

TABLE I
BIOSAR 2007 CAMPAIGN DATA SET: (X2) DENOTES THAT TWO BASELINES ARE AVAILABLE THROUGH DIFFERENT COMBINATIONS OF THE MASTER AND SLAVE TRACKS

Campaign	Scene_ID	Acquisition Date	Nr. of Tracks	Temporal Baseline (day)	Spatial Baseline (m)
BioSAR 2007	07_01xx	2007/03/09	6	32, 54	0(x2), 8(x3)
	07_02xx	2007/03/31	5		0, 8, 16, 24
	07_04xx	2007/05/02	5		0, 8, 16, 24

point [green rectangular point in Fig. 1(a)] remains unchanged, while the volume coherence $\tilde{\gamma}_V$ is shifted towards the origin byγ_{TV}.

The inversion of Pol-InSAR data contaminated by temporal decorrelation γ_{TV} leads to biased forest height estimates: The lower coherences (due to the temporal decorrelation γ_{TV}) are interpreted by the model as to be caused by higher forest heights. In other words, height estimates obtained by inverting (7) instead of (3), are overestimated depending on the level of temporal decorrelation γ_{TV}. Fig. 2(a) shows the height bias obtained by inverting (7) for different levels of temporal decorrelation ($\gamma_{\mathrm{TV}} = 0.95$ to 0.75) as a function of forest height assuming an effective vertical (interferometric) wavenumber of $\kappa_z = 0.12$ rad/m. One can clearly see that the estimation biases are significantly higher for low heights than for high heights and that the height biases increase with increasing temporal decorrelation. Note that even for low temporal decorrelation levels (on the order of 0.9) the height bias becomes critical for low forest heights.

Fig. 2(a) makes clear that for achieving acceptable height estimates temporal decorrelation has to be compensated. Unfortunately, wind-induced temporal decorrelation occurs especially in a stochastic manner within the scene [5] and can be accounted only for on the basis of detailed information about the environ-

TABLE II
TEMPOSAR 2008 AND 2009 CAMPAIGNS DATA SET: (X2) DENOTES THAT TWO BASELINES ARE AVAILABLE THROUGH DIFFERENT COMBINATIONS OF THE MASTER AND SLAVE TRACKS

Campaign	Scene_ID	Acquisition Date	Nr. of Tracks	Temporal Baseline (day)	Spatial Baseline (m)
TempoSAR 2008	08_01xx	2008/06/07	6	1, 2, 3, 5, 7, 8, 9, 10, 12, 13	-15, -5, 0, 5,10
	08_03xx	2008/06/10	6		-15, -5, 0, 5,10
	08_04xx	2008/06/12	6		-15, -5, 0, 5,10
	08_05xx	2008/06/19	6		-15, -5, 0, 5,10
	08_06xx	2008/06/20	6		-15, -5, 0, 5,10
TempoSAR 2009	09_01xx	2009/04/27	8	1(x2), 6, 7(x2), 8, 13, 14(x2), 15	-15, -10, -5, 0, 5, 10, 15
	09_02xx	2009/04/28	8		-15, -10, -5, 0, 5, 10, 15
	09_03xx	2009/05/05	6		-15, -5, 0, 5, 15
	09_04xx	2009/05/11	8		-15, -10, -5, 0, 5, 10, 15
	09_05xx	2009/05/12	8		-15, -10, -5, 0, 5, 10, 15
	09_08xx	2009/10/27	4	1, 8, 9	0, 5, 10
	09_09xx	2009/10/28	5		0, 5, 10, 15
	09_11xx	2009/11/05	1		-

TABLE III
METEOROLOGICAL INFORMATION: WIND SPEED AND PRECIPITATION. (-) DENOTES NO PRECIPITATION

TempoSAR Scene_ID	Acquisition Time		Schönharting					Nilling				
	yy:mm:dd	hh	Precipitation (mm)				Wind (m/s)	Precipitation (mm)				Wind (m/s)
			12h	24h	36h	48h		12h	24h	36h	48h	
08_01xx	2008/06/07	11	0.1	0.7	4.9	4.9	1.3-1.6	0.0	3.4	10.2	10.2	2.2
08_03xx	2008/06/10	8	-	-	-	-	0.8-1.3	-	-	0.1	4.2	0.7-0.9
08_04xx	2008/06/12	8	-	29.7	31.7	31.7	0.8-0.7	0.1	14.7	15.2	15.2	0.5-0.7
08_05xx	2008/06/19	8	-	-	-	6.5	0.8-1.0	0.1	1.9	1.9	5.5	0.6-0.7
08_06xx	2008/06/20	7	-	-	-	-	2.3-3.2	-	-	0.1	1.9	1.9-1.5
09_01xx	2009/04/27	8	-	-	-	-	1.1-0.7	-	-	-	-	1.0
09_02xx	2009/04/28	8	-	-	-	-	1.6	-	-	-	-	1.7-1.2
09_03xx	2009/05/05	8	-	1.9	10.4	10.4	1.6-1.8	0.1	1.2	7.5	7.5	0.6-1.4
09_04xx	2009/05/11	8	-	-	-	-	1.2-1.0	-	-	-	-	0.8
09_05xx	2009/05/12	8	4.1	5.1	5.1	5.1	2.0	2.1	3.3	3.3	3.3	1.5-1.6
09_08xx	2009/10/27	14	-	-	1.8	2.3	1.0-1.7	-	-	2.3	2.3	1.0-1.1
09_09xx	2009/10/28	12	0.1	0.1	0.1	0.1	0.7-0.6	0.2	0.2	0.2	0.2	0.6
09_11xx	2009/11/05	11	-	-	6.0	6.4	1.2	-	-	7.6	7.9	1.0

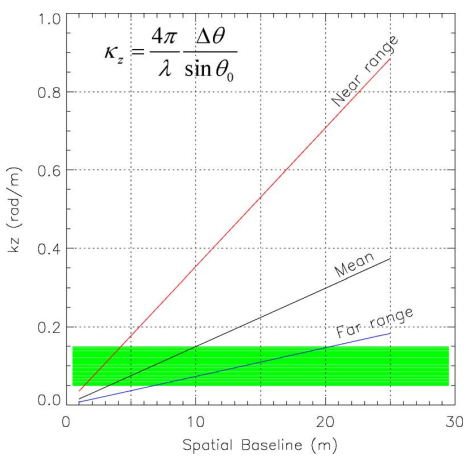

Fig. 4. Vertical wavenumber κ_z as a function of nominal baseline for L-band E-SAR system. The altitude of E-SAR is 3000 m. The incidence angle changes from 25° to 55°. Red: κ_z in near range, Blue: κ_z in far range, Black: mean κ_z from near to far range, Green: The range of κ_z between 0.05 and 0.15 rad/m.

mental conditions over the time during the two acquisitions. A valuable option to reduce the impact of nonvolumetric decorrelation contributions on the forest height estimation is to increase the volume decorrelation contribution with respect to the nonvolumetric decorrelation by increasing the spatial baseline. This is shown on the right side of Fig. 2 where the height bias obtained by inverting (7) for different levels of temporal decorrelation ($\gamma_{\mathrm{TV}} = 0.95$ to 0.75) is plotted as a function of the vertical wavenumber κ_z, assuming a constant forest height of 20 m. Even for low temporal decorrelation levels (on the order of 0.9), the height bias is critical at small baselines (12 m (i.e., 60%) for $\kappa_z = 0.05$ rad/m), but decreases with increasing baseline: for the same level of temporal decorrelation the height bias decreases to 2 m (i.e., 10%) when using a vertical wavenumber of $\kappa_z = 0.12$ rad/m. This makes clear that larger spatial baselines are of advantage in the presence of weak to moderate temporal decorrelation as they minimize the bias introduced by the temporal baseline. The price to be paid is an overall lower coherence level—due to the increased volume decorrelation contribution—that increases the phase variance of the interferometric coherence.

B. Temporal Decorrelation of the Ground Layer

For temporal baselines on the order of days and larger, temporal decorrelation contributions induced by changes in the scattering properties of the ground layer cannot be neglected

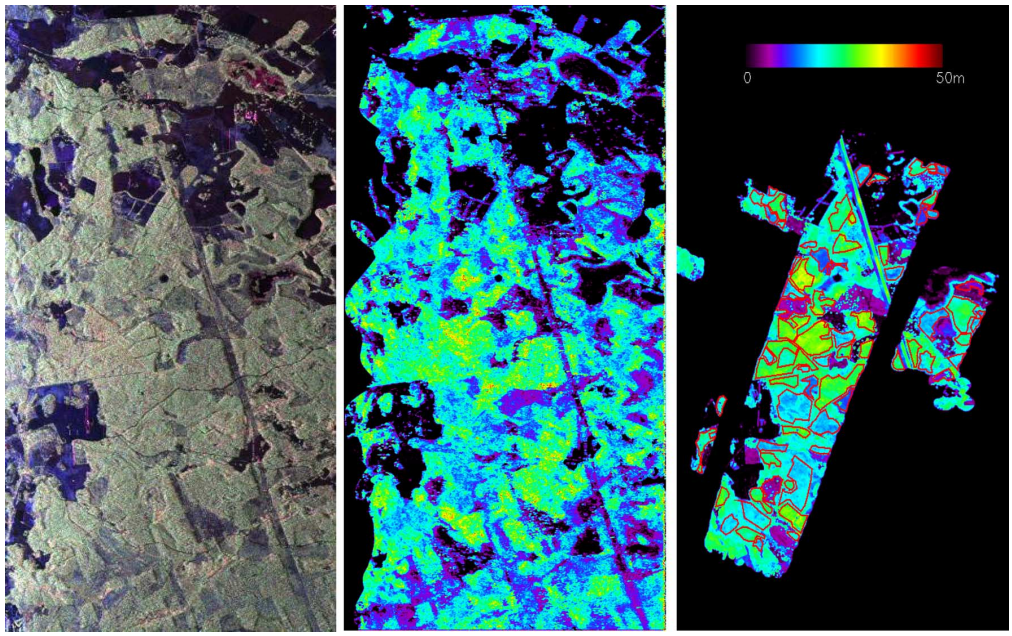

(a) (b) (c)

Fig. 5. Remningstorp test site. (a) Radar image of the Pauli components, Red: HH-VV, Green: HV, Blue: HH+VV. (b) Pol-InSAR forest height map in Remningstorp forest; scaled from 0 m to 50 m, (c) Polygons superimposed on LIDAR derived H100.

(i.e., $\gamma_{\mathrm{TG}} < 1$). The two real decorrelation contributions of γ_{TV} and γ_{TG} result in a shift of the volume decorrelation $\tilde{\gamma}_V$ and the ground point $e^{i\phi_0}$ radially towards the origin as shown in the left of Fig. 1. Note that the presence of γ_{TV} and γ_{TG} move the line-circle intersection point to $e^{i\phi_0}_{\mathrm{pseudo}}$ (blue rectangular point) and induce a ground phase error $\Delta\phi_0$. As a consequence of $\Delta\phi_0$, the phase center of volume decorrelation $\tilde{\gamma}_V$ is overestimated and leads to a height error in the Pol-InSAR inversion.

Fig. 3 shows the ground phase bias and the height bias induced by different levels of temporal decorrelation on the ground layer ($\gamma_{\mathrm{TG}} = 1.0$ to 0.8) as a function of forest height assuming a vertical wavenumber of $\kappa_z = 0.12$ rad/m and the temporal decorrelation in volume of $\gamma_{\mathrm{TV}} = 0.85$. While no ground phase bias appears for $\gamma_{\mathrm{TG}} = 1.0$, the ground phase bias $\Delta\phi_0$ increases as γ_{TG} decreases. Fig. 3(b) shows the height biases corresponding to phase biases shown on the left of Fig. 3. Compared to the impact of temporal volume decorrelation γ_{TV}, a phase bias caused by γ_{TG} introduces a smaller bias in the Pol-InSAR inversion. For example, at a forest height of 20 m, the temporal decorrelation of $\gamma_{\mathrm{TV}} = 0.85$ causes a 3 m (i.e., 15%) height bias, while the temporal decorrelation of $\gamma_{\mathrm{TG}} = 0.85$ bias to the phase error of 8° and the overestimation of about 1 m (i.e., 5%).

In Section V, the quantification of both temporal decorrelations and their impact on forest height inversion for different repeat-pass intervals will be estimated and discussed using airborne SAR data sets.

III. Temporal Decorrelation Campaigns

In order to assess the impact of temporal decorrelation, three important airborne experiments were conducted: BioSAR 2007, TempoSAR 2008, and TempoSAR 2009 campaigns. An overview of forest campaigns including the test sites and the experimental Pol-InSAR data acquired by DLR's E-SAR system [11], as well as ground measurement data is described in the following.

A. BioSAR 2007 Campaign

The BioSAR 2007 campaign was performed over the Remningstorp test site [see Fig. 5(a)] located in southern Sweden [58°28′ north, 13°38′ east). DLR's E-SAR system acquired data over the Remningstorp forest at three different dates: March 9, March 31, and May 2, 2007. During the three acquisitions, L-band Quad-polarimetric data have been acquired in a repeat-pass interferometric mode. The configurations flown and the available Pol-InSAR data sets are summarized in Table I. The experiment allows us to investigate long-term temporal baselines on the order of 32 and 54 days.

The Remningstorp forest is a part of the southern ridge of the boreal forest zone in transition to the temperate forest zone. Topography is fairly flat with some small hills and ranges between 120 m and 145 m amsl. It is a managed forest, divided into several stands with similar forest structure. Prevailing tree species are Norway spruce (*Picea abies*), Scots pine (*Pinus sylvestris*), and birch (*Betula spp.*). Forest height ranges from 5 to 35 m, with biomass levels from 50 to 300 t/ha. For the test site LIDAR data set is available for validation. 78 homogeneous stands have been delineated on the basis of LIDAR measured heights. The H100 [see Fig. 5(c)] was obtained from LIDAR height measurements by taking the maximum value of a 10 m × 10 m window corresponding to 1/100 of a hectare [17], [5]. A mean area of a stand is about 5.9 ha.

B. TempoSAR 2008 and 2009 Campaigns

The repeat-pass E-SAR system acquired fully polarimetric and interferometric SAR data over the Traunstein test site. A total of 13 radar campaigns was carried out over three different periods: five times (June 7– June 20, 2008); five times (April

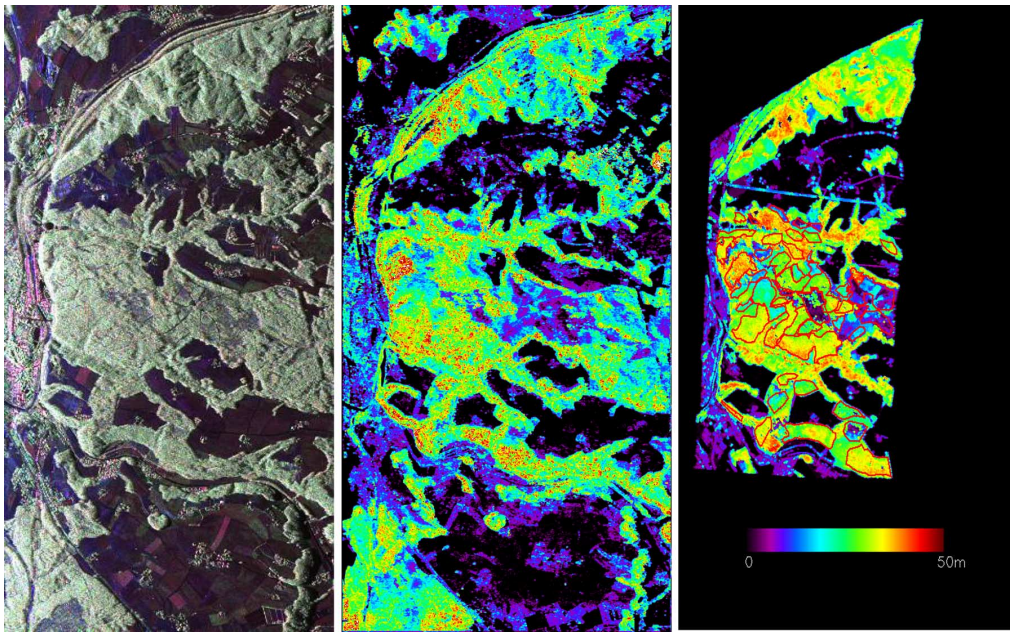

(a) (b) (c)

Fig. 6. Traunstein test site. (a) Radar image of the Pauli components, Red: HH-VV, Green: HV, Blue: HH+VV. (b) Pol-InSAR forest height map Traunstein forest; scaled from 0 m to 50 m. (c) LIDAR derived H100 overlaid with stands.

27–May 12, 2009); and three times (October 28–November 5, 2009). Fig. 6(a) shows the Pauli component images for TempoSAR 2008. From a series of Pol-InSAR acquisitions, it is possible to generate various temporal baselines up to 15 days. Thus, the TempoSAR data form a unique data set to investigate the impact of temporal decorrelation in time on Pol-InSAR inversion performance. The data sets have a sufficient number of tracks in order to perform a multibaseline approach for successful height inversion. The spatial baselines for the TempoSAR campaigns vary basically from -15 m to 15 m, with a spacing of 5 m. The available tracks and temporal/spatial baselines are summarized in Table II.

The Traunstein test site is situated in the southeast of Germany ($47^\circ 52'$ north, $12^\circ 39'$ east), about 100 km east from DLR Oberpfaffenhofen. Due to the short distance to DLR, it is easy for the E-SAR system to acquire Pol-InSAR data from Oberpfaffenhofen airport. Geologically, the test site is placed in the prealpine-moraine landscape of southern Germany. Topography varies from 600 m to 800 m amsl, with only few steep slopes. The forests are dominated by Norway spruce (*Picea abies*), beech (*Fagus sylvatica*) and fir (*Abies alba*). On a global scale this forest type is part of the temperate forest zone. It is a managed forest composed of even-aged stands which cover forest heights from 10 to 40 m. The mean biomass level is on the order of 210 t/ha while some old forest stands can reach biomass levels up to 500 t/ha. Compared to other managed forests in this ecological zone (mean biomass of 121 t/ha) the biomass values at the Traunstein test site are significantly higher. Validation of TempoSAR campaign results was based on LIDAR measurement data which was acquired on September 28, 2008. LIDAR derived H100 was shown on the right side of Fig. 6.

Meteorological data for the Traunstein test site were obtained by two local weather stations [13]. The Schönharting and Nilling stations are about 24 km northeast and northwest from the Traunstein test site. Meteorological measurements were collected at an hourly rate including air temperature (at a height of 20 and 200 cm), soil temperature (in a depth of 5 and 20 cm), relative humidity, wind velocity and precipitation during the TempoSAR campaigns. For this study, the weather data of wind speed and precipitation were used in order to check temporal changes of forest. Wind speeds from beginning to end (approximately 1 h) of each SAR acquisition are summarized in Table III. There was a relatively strong wind velocity on June 7 and June 20, 2008, with maximum wind speed of 3.2 m/s. While the wind speeds represent the values recorded at exact acquisition time, the total precipitation over the period of 12, 24, 36, and 48 h prior to the beginning of the SAR acquisition were estimated in Table III. The forest conditions on June 12, 2008 and May 12, 2009 could be wet due to significant precipitation before airborne SAR experiment.

IV. Multi-Baseline Pol-InSAR Inversion Results

Forest heights for Remningstorp and Traunstein test sites were estimated by applying an incoherent multibaseline Pol-InSAR inversion approach [12] in order to optimize the performance with respect to the actual κ_z level. For the E-SAR acquisition geometry, the radar incidence angle θ_0 varies form 25° to 55° [11], [5] implying a variation of the vertical wavenumber from near to far range, up to a factor of five. Fig. 4 shows the vertical wavenumbers κ_z of the L-band E-SAR acquisition as a function of nominal spatial baseline, assuming the altitude of E-SAR of 3000 m. The vertical wavenumber range for each spatial baseline for the BioSAR 2007 and TempoSAR campaigns is obtained by using the nominal spatial baseline values given in Tables I and II. An optimum inversion performance across whole range can be achieved by combining the optimum range of the multiple available baselines. Accordingly, regions with low inversion performance caused

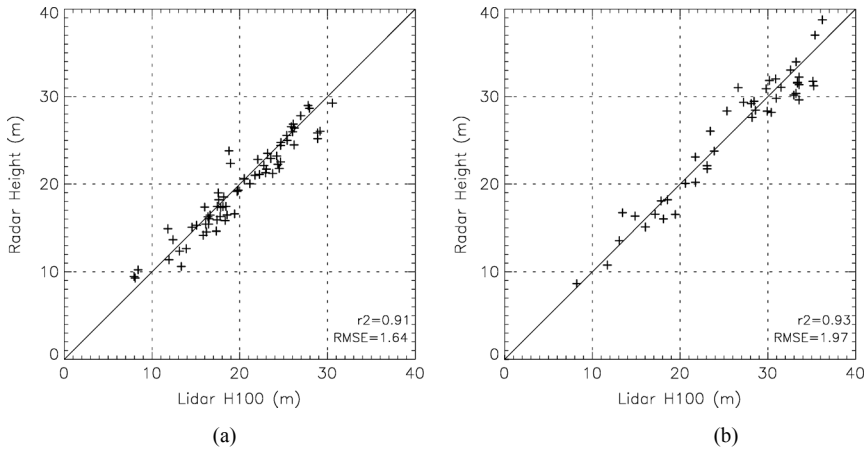

Fig. 7. Validation plots: LIDAR reference height vs. multibaseline Pol-InSAR forest height estimates for Remningstorp (a) and Traunstein (b) test sites.

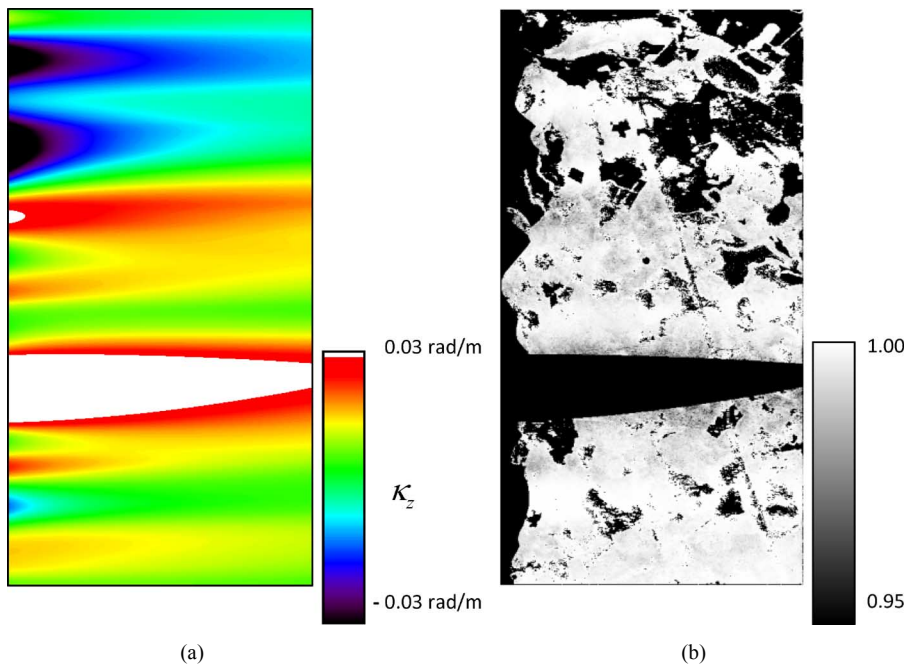

Fig. 8. Left: The vertical wavenumber at zero nominal spatial baseline, scaled from -0.03 to 0.03 rad/m. White and black indicate the vertical wavenumber characterized by larger than 0.03 and smaller than -0.03. Right: The volume decorrelation obtained by the forest height in Fig. 5 and the vertical wavenumber from left image assuming the mean extinction of $\sigma = 0$ dB/m, scaled from 0.95 to 1.00. Areas with the absolute vertical wavenumber larger than 0.03 and nonforest part are masked out (black).

by too high and too low volume sensitivity characterized by a vertical wavenumber larger than 0.15 and smaller than 0.05 are masked out for each individual baseline [5]. Also areas with a coherence level lower than 0.3 are masked out where accurate inversion cannot be expected for a reasonable number of looks. Height estimation accuracy is finally used to select the best estimate from multibaseline inversion results by using a criterion (i.e., the minimum value) defined by the conventional interferometry height accuracy, the amplitude of coherence and the vertical wavenumber [12].

For the Remningstorp test site the multibaseline Pol-InSAR inversion was done on the data set acquired on March 31, 2007 and validated against H100. Fig. 5 in the middle shows the obtained forest height map, scaled from 0 m to 50 m. The validation plot is shown on the left side of Fig. 7 where a correlation coefficient r^2 of 0.91 with a root mean square error (RMSE) of 1.64 m is reached. The correlation between LIDAR and radar height measurements is highly significant within 10%.

For the Traunstein test site forest heights have been estimated for two data sets acquired in 2008 and 2009. Height estimates for the TempoSAR 2008 data set (acquired on June 12, 2008) are validated against LIDAR measurements (i.e., H100) acquired in two months after the SAR campaign. The Pol-InSAR forest height map is shown in the middle of Fig. 6 and on the right the LIDAR measurement used for validation. Both height maps are also scaled from 0 m to 50 m. A comparison of Pol-InSAR forest heights against LIDAR measurements is shown in Fig. 7 (on the right) whereas the correlation coefficient r^2 reaches 0.93 with a RMSE of 1.97 m, covering a height range from 10 to 35 m. At the same time, mean extinction coefficients have been estimated

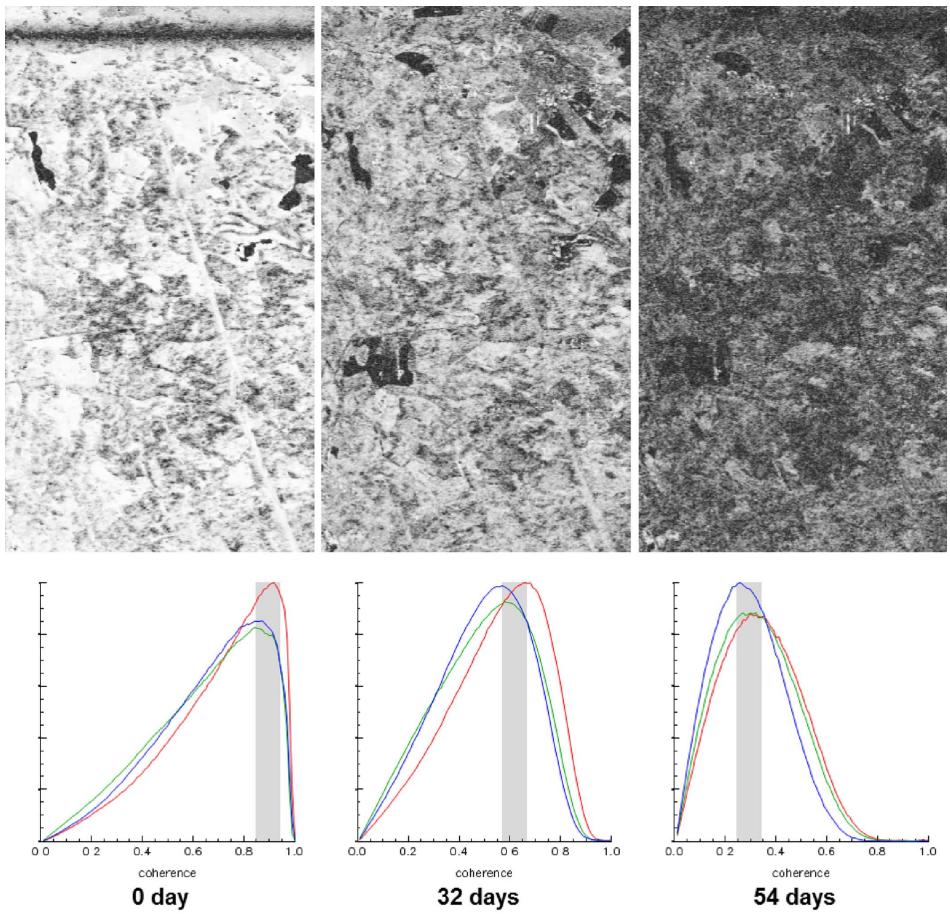

Fig. 9. (Top) HH Coherence maps. Bottom: Coherence histograms (of forested area) for a 0-, 32-, and 54-day temporal baselines in Remningstorp test site in different polarizations; HH (red), HV (green), and VV (blue). Grey columns are of the highest frequency at different polarizations in coherence histograms.

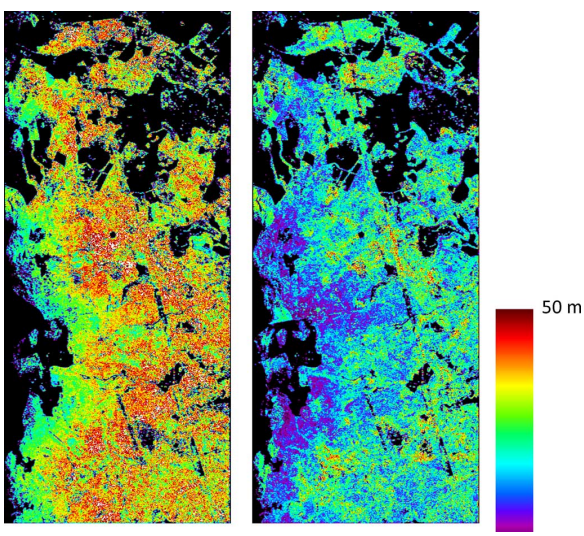

Fig. 10. Forest height map and height bias for Remningstorp forest, scaled 0 m to 50 m. Left: Inversion height map with one month temporal baseline, Right: Different height map between left image and the middle image of Fig. 5.

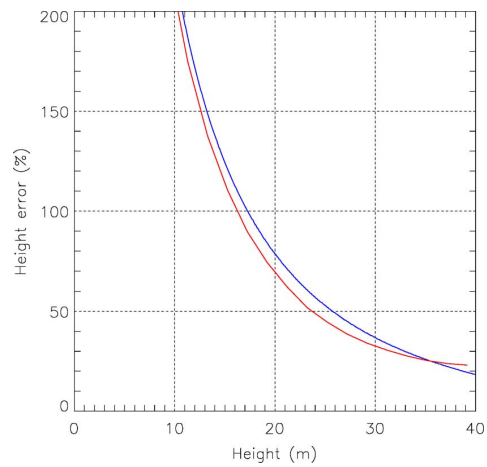

Fig. 11. Height error (%) versus forest height for Remningstorp test site. Red: Estimated height error on 32-day temporal baseline (temporal decorrelation $\approx$ 0.65). Blue: Simulated height bias with temporal decorrelation on the order of 0.65 as Fig. 2(a).

for the Traunstein test site. The extinctions vary mainly from 0 to 0.5 dB/m with a median value of 0.14 dB/m.

The results of both test sites demonstrate that multibaseline Pol-InSAR forest height inversion provides consistent forest height maps for different type of forests in the case of small temporal baselines (on the order of minutes). In the next section, the impact of temporal decorrelation is evaluated from the multibaseline inversion results.

V. Assessment of Temporal Decorrelation

In this section the impact of temporal decorrelation on Pol-InSAR inversion performance is quantitatively estimated and

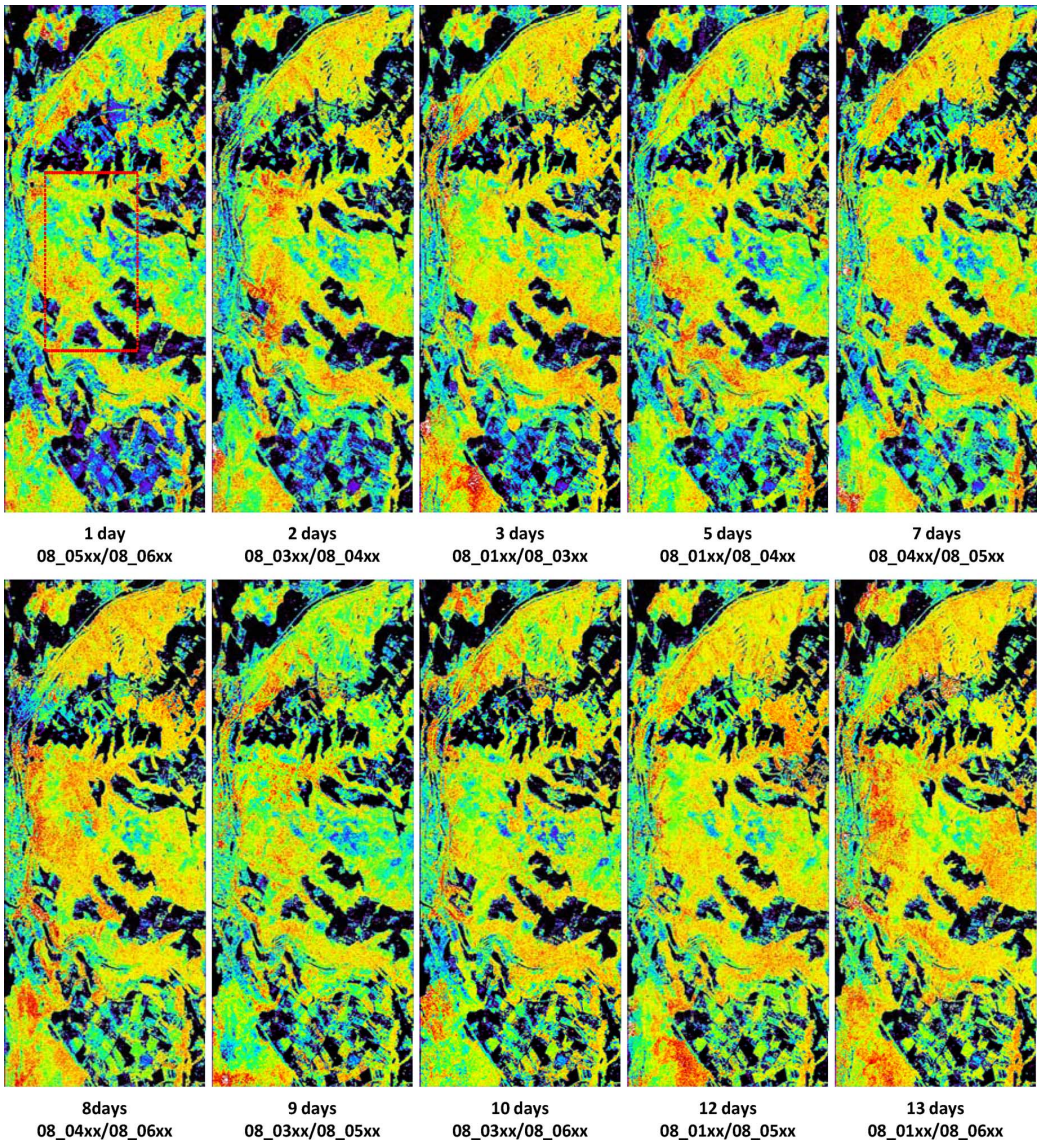

Fig. 12. Forest height maps for TempoSAR 2008 campaign with temporal baselines from 1 to 13 d; scaled 0 m to 50 m; color table in Fig. 5. Forest heights with temporal decorrelation on the order of days are overestimated compared to the multibaseline Pol-InSAR inversion result shown in Fig. 6.

analyzed. Two different approaches are proposed to quantify the temporal decorrelation and its impact on forest parameter inversion. The simplest way to quantify temporal decorrelation at a given temporal baseline is to avoid any (spatial) baseline induced decorrelation contribution (e.g., volume decorrelation) by using a "zero spatial baseline" configuration and compensating for system induced decorrelation effects (e.g., SNR decorrelation). In this special case of a zero spatial baseline interferogram (i.e., $\kappa_z = 0$ and $\tilde{\gamma}_V = 1$), temporal decorrelation can be directly estimated from (7) [5], [9], [15]. The second approach is based on the estimation of the height error induced by temporal decorrelation at nonzero multispatial baselines (i.e., $\kappa_z \neq 0$ and $\tilde{\gamma}_V < 1$). It has the advantage of establishing a direct relationship between temporal decorrelation level and the height error. And, it also allows at the same time the estimation of the individual temporal decorrelation levels of γ_{TV} and γ_{TG}. For this, it is necessary to have information on forest height and mean extinction. In this case, both parameters are obtained by means of multibaseline Pol-InSAR inversion [12] using only small temporal baselines assumed free of temporal decorrelation as shown in Section IV. The results are then used to assess the height error induced by the individual temporal baselines and to estimate temporal decorrelation levels of γ_{TV} and γ_{TG} as a function of temporal baseline.

As summarized in Tables I and II, the BioSAR 2007 and TempoSAR campaigns have a variety of temporal baselines varying from minutes, days, and weeks, up to 54 days. In this study, temporal baselines are categorized into three time scale classes; long-term (weeks to months), mid-term (day to weeks) and short-term (minutes to hours) temporal baselines. The results about temporal decorrelation at different time scales are discussed in the next sections.

A. Long-Term Temporal Baseline: Weeks to Months

To investigate the temporal decorrelation at long-term temporal baselines, the data sets of the BioSAR 2007 campaign were selected where three different acquisitions provide long-term temporal baselines on the order of about one and two months.

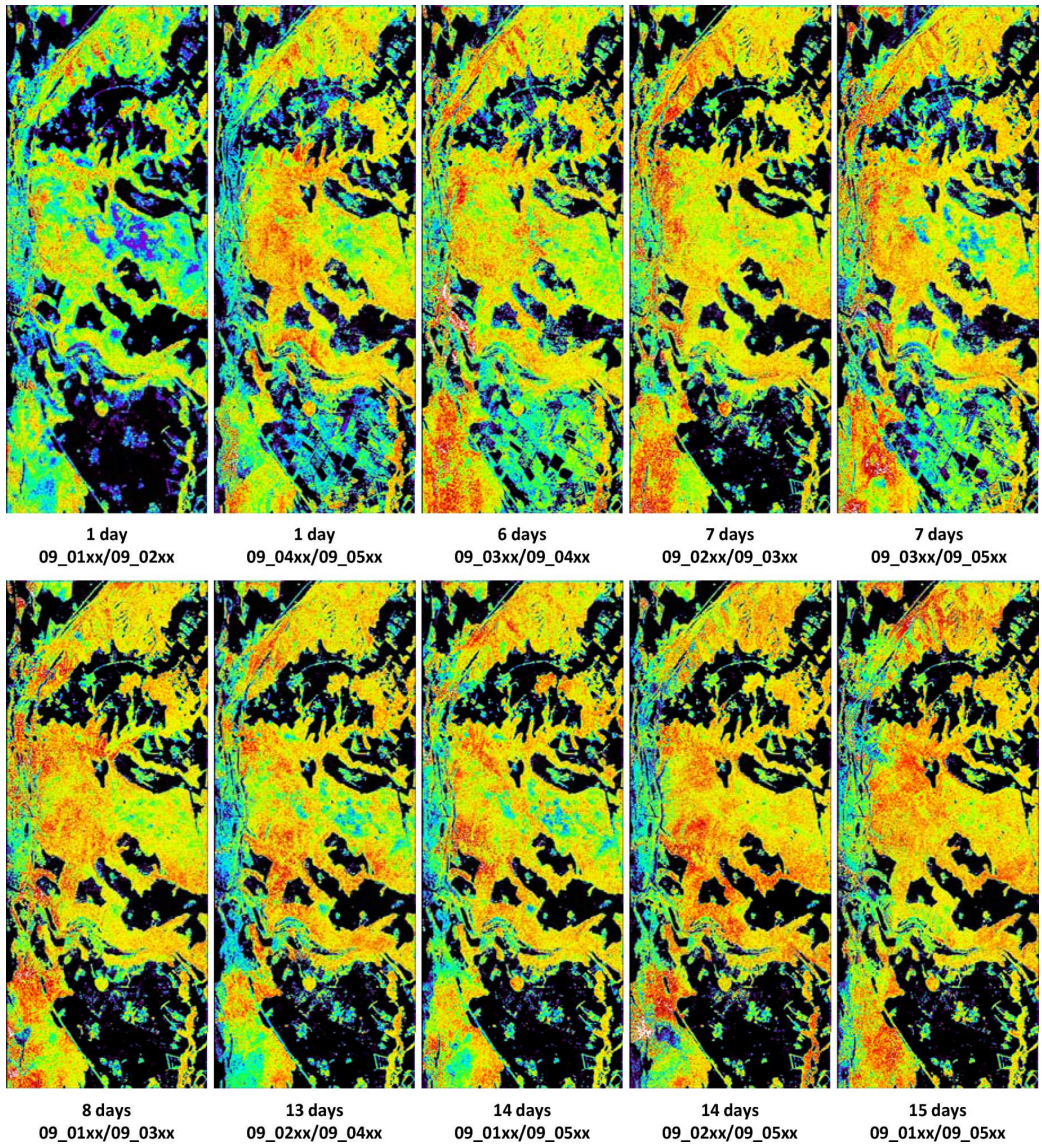

Fig. 13. Forest height maps for TempoSAR 2009 campaign with temporal baselines from 1 to 15 d; scaled 0 to 50 m; color table in Fig. 5. Forest heights are with temporal decorrelation on the order of days are overestimated compared to the multibaseline Pol-InSAR inversion result shown in Fig. 6.

As mentioned, the straightforward way to quantify temporal decorrelation is to use a zero spatial baseline configuration. Acquisitions at zero spatial baseline were used by selecting the forested areas within the scene where the spatial baseline is if not zero at least sufficiently small (i.e., $|\kappa_z| < 0.03$). Fig. 8(a) shows an image of κ_z at zero nominal spatial baseline, scaled from -0.03 to 0.03 rad/m. Regions with a vertical wavenumber larger than 0.03 and smaller than -0.03 are not considered and masked out. The volume decorrelation of the remaining areas is simulated by the forest height information available [see Fig. 5(b)] assuming a mean extinction $\sigma = 0$ dB/m. Fig. 8(b) shows the volume decorrelation of the relevant areas (i.e., $|\kappa_z| < 0.03$), scaled from 0.95 to 1.00. The volume decorrelations are nearly unity with an average level of 0.999. Accordingly, the approach eliminates all baseline induced decorrelation sources so that the loss in coherence is only due to temporal decorrelation.

Temporal decorrelation maps (HH polarization) for a zero spatial baseline are shown in Fig. 9. At the bottom of Fig. 9, the coherence histograms for HH (red), HV (green), and VV (blue) polarizations over the forested areas in the scene are shown for three different temporal baselines. As expected, the impact of temporal decorrelation increases with increasing temporal baseline in all polarizations. Even for the 0-day case acquired with a temporal baseline shorter than 1 h, the loss in coherence indicates the presence of temporal decorrelation: The temporal decorrelation levels are on the order of 0.65 for 32 days and 0.30 for the 54 days. The coherence level for 54 days was already so low that almost the entire image is covered by the nonvalid coherence mask.

Pol-InSAR inversion with a temporal baseline of 32 days was performed using the nonzero spatial baselines. The inversion result and height bias (overestimation) are shown in Fig. 10. In this case, the obtained forest heights are fairly overestimated all over the image [compared to Fig. 5(a)] due to the temporal decorrelation. The height error introduced by temporal decorrelation can be estimated by

$$\text{Height error}(\%) = \frac{\Delta h_v}{h_v} \times 100 \tag{8}$$

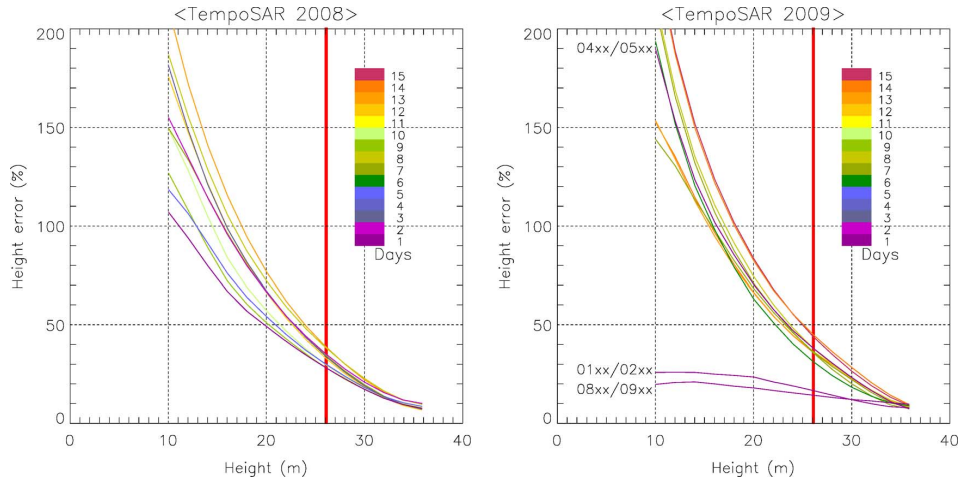

Fig. 14. Height error (%) versus forest height for temporal baselines from 1 to 15 d; Color-coding represents the temporal baselines. (a) Height error for TempoSAR 2008. (b) Height error for TempoSAR 2009. Red line represents the mean forest height of 26 m in the rectangle in Fig. 12.

where h_v is the forest height from multibaseline inversion [see Fig. 5(b)] and Δh_v the height bias (overestimation) introduced by the uncompensated temporal decorrelation [see Fig. 10(right)]. The estimated height error for the 32-day temporal baseline is plotted in Fig. 11. The red line represents the estimated height error for a 32-day temporal baseline while the blue line shows the simulated height bias (as shown in Fig. 2(a) in Section II-A) obtained by inverting (7) for $\gamma_{\mathrm{TV}} = 0.65$ corresponding to the mean temporal decorrelation as obtained from the histograms for the 32-day temporal baseline in Fig. 9. There is a clear tendency of increasing height error with decreasing forest height in accordance with the simulation shown in Fig. 2. Lower forest stands are much more affected by uncompensated volumetric decorrelation contributions than higher forest stands. The level of temporal decorrelation with one month repeat-pass time interval still allows applying Pol-InSAR height inversion, but it introduces a large height bias, especially in low forest stands.

B. Mid-Term Temporal Baseline: Day to Weeks

Temporal decorrelation at mid-term temporal baselines (on the order of days up to weeks) is now investigated and quantified. During the TempoSAR 2008 and 2009 campaigns, Pol-InSAR data were acquired 13 times distributed over a period of 15 days. This allows to form interferograms with temporal baselines ranging from 1 up to 15 days (see Table II).

Forest height maps have been estimated by using multibaseline Pol-InSAR inversion [12]; the inversion results are shown in Figs. 12 and 13. As expected, forest heights were clearly overestimated when compared to the forest height shown in the middle of Fig. 6. In general, overestimation increases with increasing temporal baseline. The height errors for TempoSAR 2008 and 2009 are estimated using (8) and are shown in Fig. 14. The color-coding indicates the temporal baselines ranging from 1 to 15 days. The inversion error increases with decreasing forest height and increasing temporal baseline, similar to the results obtained in the previous section. Note that the height errors obtained from the different 1-day temporal baselines can be fairly different as shown in Fig. 14(b). The acquisition pairs (09_01xx/09_02xx and 09_08xx/09_09xx) for TempoSAR 2009 [see Fig. 14(b)] lead to 10–25% height error depending on forest heights, while the pair (09_04xx/09_05xx) acquired also with 1-day temporal decorrelation leads to much larger height errors of 20–200%, due to the rather unstable weather conditions (e.g., wind and/or precipitation) during the acquisitions. In the following, both temporal decorrelations of γ_{TV} and γ_{TG} will be estimated by using nonzero multibaseline Pol-InSAR data and be discussed with meteorological information.

1) Temporal Decorrelation on the Ground Layer γ_{TG}: As discussed in Section II-B, the temporal decorrelation on the ground γ_{TG} biases the estimate of the ground phase and leads to an overestimation of forest height. It is hard to estimate the impact of γ_{TG} by means of a "zero spatial baseline" because of no phase difference of interferograms at different polarizations. Using the reference forest height h_v and a mean extinction σ (obtained in Section IV) from multibaseline Pol-InSAR inversion, the volume decorrelation $\tilde{\gamma}_V(h_v, \sigma, \kappa_z, \theta_0)$ is calculated from (2) (by setting $\phi_0 = 0$) and plotted [corresponding to the green circle in Fig. 1(b)]. For any Pol-InSAR acquisition, the associated volume-only coherence $\tilde{\gamma}(\vec{w}_{m=0})$ and the biased ground point $e^{i\phi_0}_{\mathrm{pseudo}}$ are obtained. The ground phase error $\Delta\phi_0$ is estimated by the phase difference between $\tilde{\gamma}_V(h_v, \sigma, \kappa_z, \theta_0)$ and $\tilde{\gamma}(\vec{w}_{m=0})e^{-i\phi_0}_{\mathrm{pseudo}}$. Temporal decorrelation on the ground layer γ_{TG} is obtained by the x-intercept of the line defined by $\tilde{\gamma}(\vec{w}_{m=0})e^{-i\phi_0}_{\mathrm{pseudo}}e^{-i\Delta\phi_0}$ and $e^{-i\Delta\phi_0}$ [red circle and blue rectangular points in Fig. 1(b)]

$$\gamma_{\mathrm{TG}} = \mathrm{Re}\left(\tilde{\gamma}(\vec{w}_{m=0})e^{-i\phi_0}_{\mathrm{pseudo}}e^{-i\Delta\phi_0}\right) - \mathrm{Im}\left(\tilde{\gamma}(\vec{w}_{m=0})e^{-i\phi_0}_{\mathrm{pseudo}}e^{-i\Delta\phi_0}\right) \Big/ \tan\theta_{\mathrm{gr}} \quad (9)$$

where $\tan\theta_{\mathrm{gr}}$ represents the gradient of the line.

The quantitative estimation of γ_{TG} for the Traunstein test site (corresponding to the red rectangle in Fig. 12) is performed using Pol-InSAR data sets acquired during the TempoSAR 2008 and 2009 with temporal baselines up to 15 days. Fig. 17 shows the mean estimated temporal decorrelation γ_{TG} plotted against all possible TempoSAR 2008 and 2009 temporal

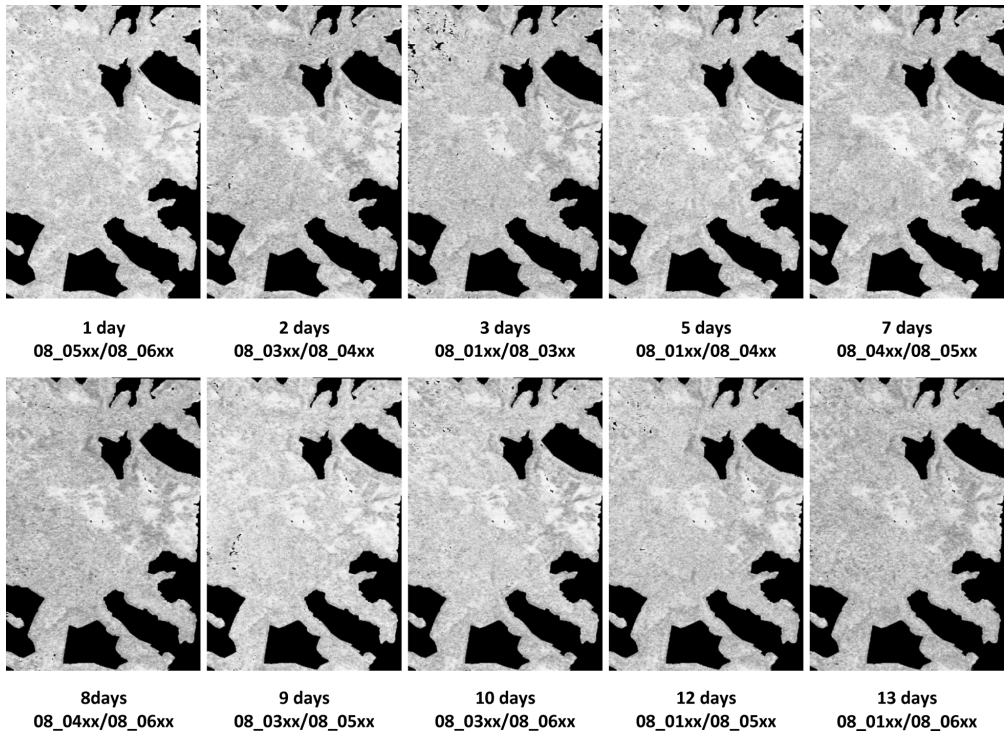

Fig. 15. Temporal decorrelation on the ground layer γ_{TG} for TempoSAR 2008 campaign from 1- to 13-day temporal baseline, scaled from 0 (black) to 1 (white); Section of Traunstein test site—red dotted rectangle in Fig. 12.

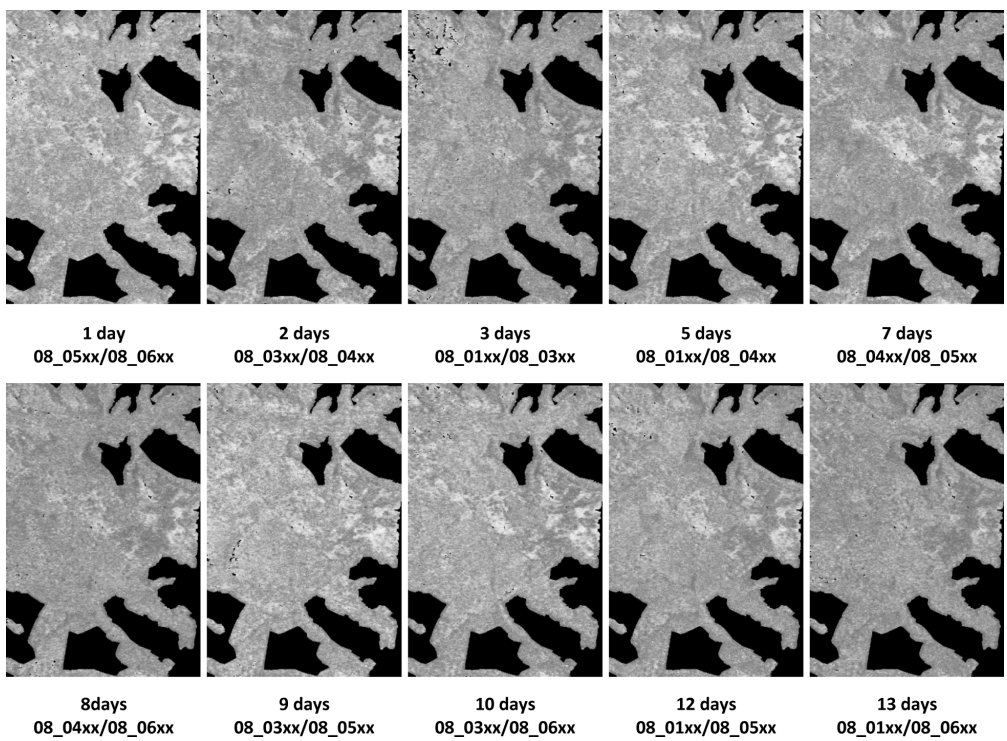

Fig. 16. Temporal decorrelation in volume γ_{TV} for TempoSAR 2008 campaign from 1- to 13-day temporal baseline, scaled from 0 (black) to 1 (white); Section of Traunstein test site—red dotted rectangle in Fig. 12.

baselines. The asterisks represent the averaged temporal decorrelations γ_{TG} for TempoSAR 2008 and the rectangles the ones for TempoSAR 2009. Temporal decorrelation γ_{TG} decreases from 0.91 to 0.68 with increasing temporal baseline. However, comparing on the three 1-day baseline results of TempoSAR 2009 (Sence_ID: 09_01xx/09_02xx, 09_04xx/09_05xx, and 09_08xx/09_09xx), the level of γ_{TG} for the 09_04xx and 09_05xx pair is much lower ($\gamma_{\mathrm{TG}} = 0.76$). This can be due to a change in the dielectric properties of the ground induced, for example, by precipitation. Indeed, during the TempoSAR

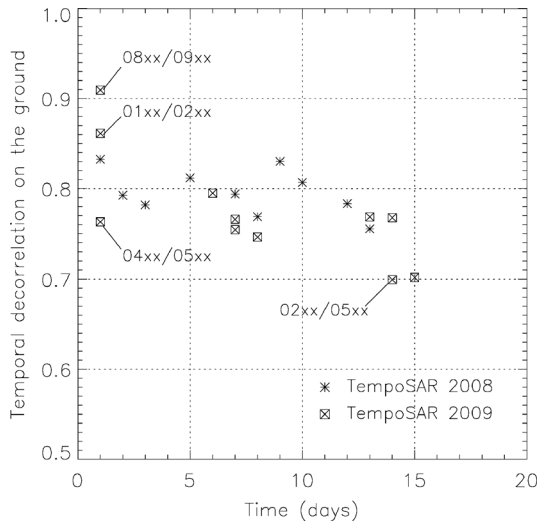

Fig. 17. Mean temporal decorrelations γ_{TG} on the ground layer against temporal baseline up to 15 days for TempoSAR 2008 and 2009; Section of Traunstein test site—red dotted rectangle in Fig. 12. Asterisk point: TempoSAR 2008 and rectangular point: TempoSAR 2009.

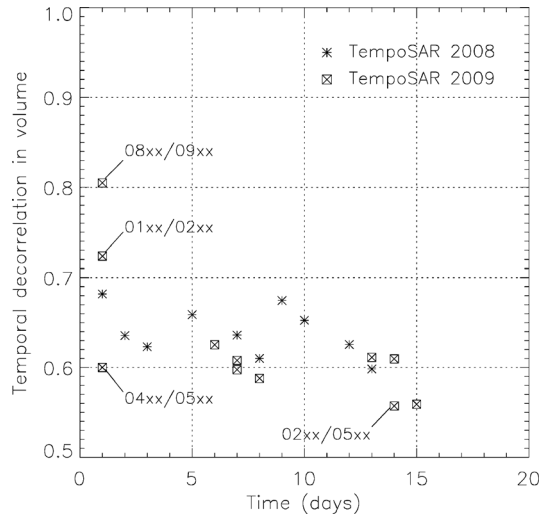

Fig. 18. Mean temporal decorrelations γ_{TV} in volume against temporal baseline up to 15 days for TempoSAR 2008 and 2009; Section of Traunstein test site—red dotted rectangle in Fig. 12. Asterisk point: TempoSAR 2008 and rectangular point: TempoSAR 2009.

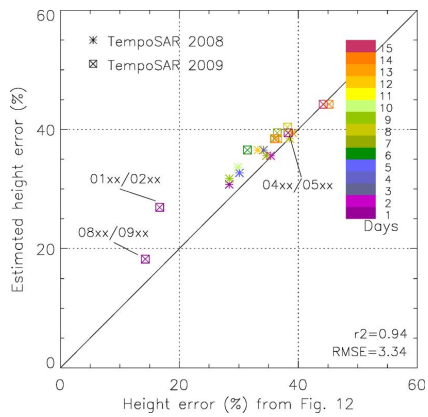

Fig. 19. Validation of the estimated height error. X-axis: Height error on a mean forest height of 26 m from Fig. 14. Y-axis: Height error estimated by inverting (6) with temporal decorrelation γ_{TG} on the ground layer from Fig. 17 and temporal decorrelation γ_{TV} in volume from Fig. 18. Color-coding represents the temporal baselines. Asterisk point: TempoSAR 2008 and rectangular point: TempoSAR 2009.

2009 campaign, there was a 4.1 mm rain event just before the 09_05xx acquisition on May 12, 2009 (see Table III) changing probably the dielectric properties of the ground layer. Therefore, γ_{TG} values estimated by the interferometric pairs including track 09_05xx (i.e., 09_04xx/09_05xx, and 09_02xx/09_05xx) at temporal baselines of 1 and 14 days show much lower coherence levels than those without the 09_05xx acquisition at same temporal baselines (i.e., 09_01xx/09_02xx, 09_08xx/09_09xx, and 09_01xx/09_04xx) as shown in Fig. 17. This is a significant result indicating that precipitation is critical affecting the temporal stability of the ground.

2) Temporal Decorrelation in Volume Layer γ_{TV}: Temporal decorrelation γ_{TV} for temporal baselines on the order of days depends on short term changes of the dielectric properties of the volume (and the ground) and on the rather stochastic (wind-induced) motion. As mentioned in Section II-A, temporal decorrelation of the volume γ_{TV} reduces the amplitude of the volume decorrelation $\tilde{\gamma}_V$ in (6). Accordingly, γ_{TV} can be estimated from the amplitude ratio of $\tilde{\gamma}_V(h_v, \sigma, \kappa_z, \theta_0)$ and $\tilde{\gamma}(\vec{w}_{m=0}) e^{-i\phi_0}_{\mathrm{pseudo}} e^{-i\Delta\phi_0}$ [corresponding to the green and red circle points in Fig. 1(b)].

The estimated temporal decorrelation coefficients γ_{TV} for all temporal baselines in TempoSAR 2008 are shown in Fig. 16 making two main points obvious: The first one is that temporal decorrelation γ_{TV} tends to decrease with increasing temporal baseline, but faster than γ_{TG} as shown in Fig. 15. The second point is that the decrease of γ_{TV} is not necessarily monotonic in time and space. It depends not only on the random behavior of wind-induced motion but also on different levels of water content (e.g., dielectric constant) in the volume due to precipitation and vaporization. Fig. 18 shows the averaged temporal decorrelation γ_{TV} for all temporal baselines up to 15 days. Temporal decorrelation γ_{TV} tends to decrease with increasing temporal baseline similar to temporal decorrelation γ_{TG}. For temporal baselines of a few days a rapid drop of coherence level going along with a large variation of coherence levels can be observed. The lower values of γ_{TV} at temporal baselines of 1 day (09_04xx/09_05xx) and 14 days (09_02xx/09_05xx) result from the changes of dielectric properties of the scatterers in the volume layer due to the precipitation event on May 12, 2009 (see Table III).

For the validation of the obtained results, a simulated height error for the estimated γ_{TG} and γ_{TV} obtained from each temporal baseline for a κ_z of 0.1 rad/m and a forest height of 26 m (mean forest height value within red rectangle in Fig. 12) is calculated and plotted against the real height error on height of 26 m in Fig. 14. Fig. 14 shows this plot: on the x-axis is the real height error while on the y-axis the simulated height error obtained by using the estimated temporal decorrelations (γ_{TV} and γ_{TG}) from Figs. 17 and 18 are given. Asterisks and rectangles indicate the height errors (%) for TempoSAR 2008 and 2009 and the color-coding indicates the temporal baseline, from 1 to 15 days. For example, a height error of 18% is estimated corresponding to $\gamma_{\mathrm{TV}} = 0.80$ and $\gamma_{\mathrm{TG}} = 0.91$ at a temporal baseline on the order of 1 day (09_08xx/09_09xx),

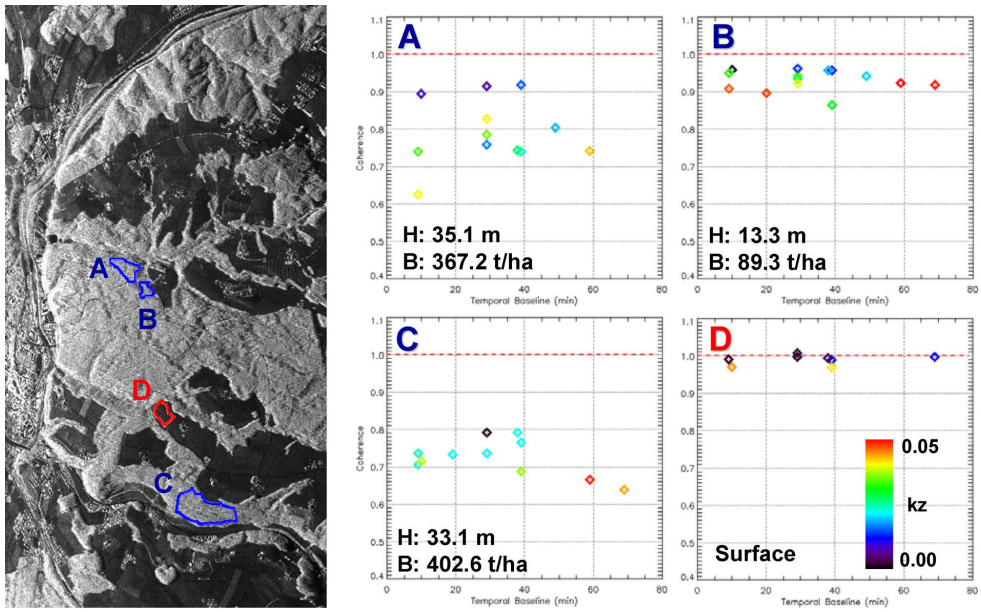

Fig. 20. (Left) Amplitude image of the Traunstein test site in HH polarization with positions of the investigated forest stands. (A), (C) High forest (blue). (B): Low forest (blue). (D) Field (red). (Right) Coherence versus temporal baseline (in minutes) plots for each of the selected areas A, B, C, and D; Color of point represents vertical wavenumber κ_z (see legend bottom right).

while a 14% height error is obtained for a height of 26 m in Fig. 14(b). However, temporal decorrelations on the order of $\gamma_{\mathrm{TV}} = 0.60$ and $\gamma_{\mathrm{TG}} = 0.76$ at another 1-day temporal baseline (09_04xx/09_05xx) result in stronger height errors of 39% due to the precipitation between two acquisitions. In this case, the value in Fig. 14 is quite similar indicating a height error of 38%. The comparison of temporal decorrelations and height errors shows a surprisingly high r^2 of 0.94 with an RMSE of 3.34%. This means that the modeling of γ_{TV} and γ_{TG} is in accordance with the experimental results achieved.

C. Short-Term Temporal Baseline: Minutes to Hours

Pol-InSAR acquisitions with DLR's E-SAR system operating in a repeat-pass mode can be realized with minimum temporal baselines on the order of 10–15 min depending on the dimension of the scene acquired. In the frame of the TempoSAR 2008 campaign, temporal baselines vary usually from 10 min up to 1 h with a maximum of 74 min. In this case, temporal baselines are short enough to ignore the temporal decorrelation on the ground layer (i.e., $\gamma_{\mathrm{TG}} = 1$).

In the following the behavior of temporal decorrelation in the volume γ_{TV} for short-term temporal baselines is investigated by using (7). In order to reduce volume decorrelation ($\tilde{\gamma}_V \cong 1$) and isolate temporal decorrelation effects, only interferometric pairs with small vertical wavenumber values ($\kappa_z < 0.05$) have been selected.

To investigate the behavior of coherence for short-term temporal baselines and very small spatial baselines, three forested stands and one bare field were selected. The forest stands were selected using the ground measurements in order to get uniform stands in terms of forest height and biomass [14]. Fig. 20(left) shows the HH amplitude image of the Traunstein test site indicating the four selected areas. Stand A and C are characterized by higher forest height and biomass (A: 35.1 m, 367.2 t/ha, and C: 33.1 m, 402.6 t/ha), while the height of stand B is rather low (B: 13.3 m, 89.3 t/ha). The bare field D is used as a reference.

The plots in Fig. 20 on the right show the variation of coherence over the selected areas as a function of vertical wavenumber (color) and temporal baseline. The color-coding indicates the average vertical wavenumber κ_z per stand and the x-axis shows the temporal baseline. Plot D for the bare field shows a high coherence level for all spatial and temporal baselines indicating a high temporal stability at least for the observed period of 74 min. In contrast, volume scatterers decorrelate at short-term temporal baseline (see Fig. 20 plots A, B, and C), where decorrelation is caused by wind-induced motion. Especially the changes in coherence at the taller forests stands (plot A and C) are significant. To exclude any impact of remaining volume decorrelation on the interpretation of the results, only the behavior of acquisitions with very similar vertical wavenumber is discussed. Due to the variation of κ_z within each interferogram not all available interferograms can be used for all stands. In plot A, a strong variation of coherence, independent of temporal baseline, can be observed. Coherences in plot B (low forest case) have less variation than those in plot A. Similar vertical wavenumbers κ_z (red points) maintain the coherence level up to 60 min. Plot C shows coherences with similar spatial baseline (sky blue points) with a maximum coherence after 40-min temporal baseline. Comparing the observations from plot A, B and C, wind-induced temporal decorrelation effects over forested regions seem to be of random nature.

Fig. 21 shows the impact of wind-induced temporal decorrelation on forest height estimates. Multibaseline Pol-InSAR inversion results from five acquisition dates in 2008 (see Tables II and III) are connected to wind speed measurements. Wind speed measurements were taken from two meteorological stations (Nilling and Schönharting) close to the Traunstein test site and are shown in Fig. 21(bottom) and Table III. Height

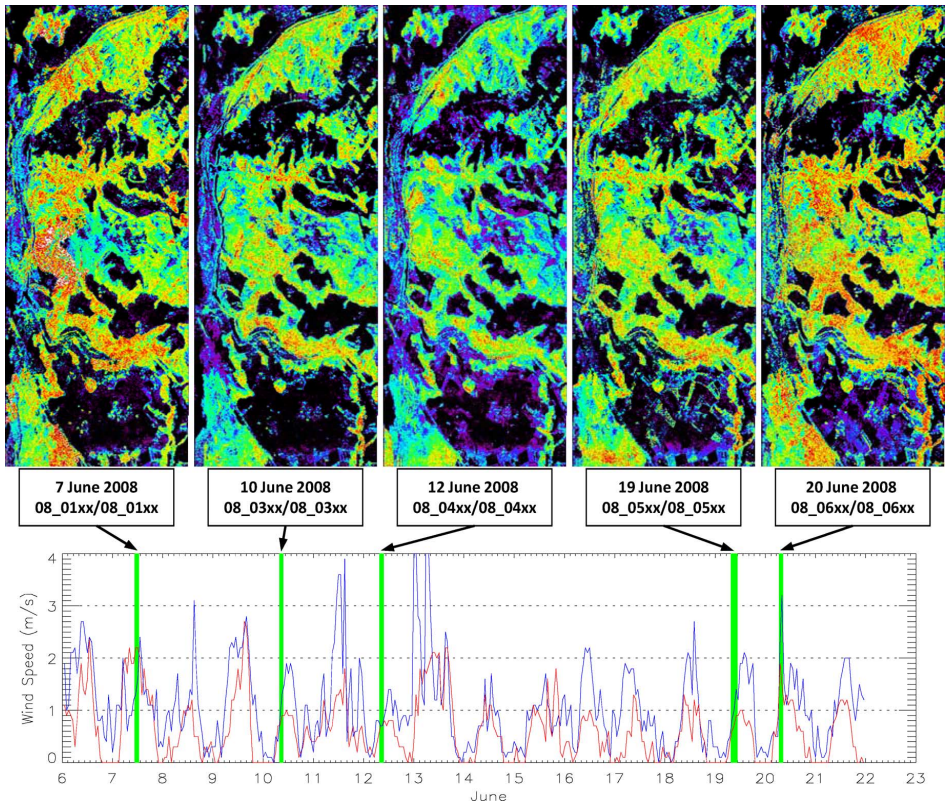

Fig. 21. Impact of wind-induce temporal decorrelation on forest height estimates. The stronger wind causes the more bias in Pol-InSAR inversion. (Top) Forest height maps from five different acquisition dates in TempoSAR 2008, scaled 0 to 50 m. (First row) Acquisition date. (Second row) Scene_ID in Table III. (Bottom) Wind speed during TempoSAR 2008 campaign. Red: Schönharting station, Blue: Nilling station, and Green: Acquisition time.

estimates from acquisitions with wind speeds of up to 2 m/s are significantly higher (08_01xx and 08_06xx in Fig. 21) than height estimates where wind speed was below 1 m/s (08_03xx, 08_04xx, and 08_05xx in Fig. 21). Fig. 21 shows the impact of weather (wind) condition on forest height estimates by means of repeat-pass SAR systems. Reliable heights were obtained only for acquisitions on June 10 and 12, 2008, with less wind (mean wind speed less than 1 m/s).

VI. Discussion and Conclusion

In order to successfully perform Pol-InSAR forest structure parameter estimation, the characterization of temporal decorrelation over forest is essential for the design of airborne SAR campaigns and much more for the implementation of future spaceborne missions operating in a repeat-pass mode. In this paper, the impact of temporal decorrelation on Pol-InSAR forest height inversion performance has been addressed and temporal decorrelation as a function of temporal baseline has been investigated for a wide range of temporal baselines. Different temporal decorrelations for the volume and the ground layer have been incorporated into the two-layer (volume/ground) RVoG scattering model, in order to account for the different decorrelation behaviors. Both decorrelations bias the Pol-InSAR inversion results, but in a different way: While volume temporal decorrelation γ_{TV} reduces the amplitude of the volume decorrelation contribution, temporal decorrelation γ_{TG} on the ground layer introduces a ground phase error. Both effects lead to an overestimation of forest heights. This phase error is the key idea for estimating the temporal decorrelation γ_{TG} of the ground layer.

The Pol-InSAR data sets acquired in BioSAR 2007 and TempoSAR 2008 and 2009 campaigns were used for the quantitative assessment of temporal decorrelation for temporal baselines ranging from 10 min up to 54 days. The impact of temporal decorrelation has been separately assessed on three different levels of temporal baseline: long-term (months—weeks), mid-term (weeks–day) and short-term (hour–minutes) temporal baselines.

The level of temporal decorrelation (0.3) with 54-day repeat-pass time of BioSAR 2007 data makes Pol-InSAR applications not possible due to by the nonvalid coherence mask. In the case of 32-day temporal baseline, the level of coherences in forest was higher than 0.3 so that Pol-InSAR inversion was still able to be applied but forest height was quite overestimated due to the uncompensated temporal decorrelation. The decorrelation level is sufficient to cause height error on the order of 20–200% depending on forest heights and spatial baseline setup.

Using multibaseline Pol-InSAR data sets acquired during the TempoSAR campaigns with temporal baselines on the order of 1 day, up to 2 weeks (15 days), it is possible to estimate the different temporal decorrelation contribution γ_{TV} and γ_{TG}. Both γ_{TV} and γ_{TG} tend to decrease with increasing temporal baseline. However, the decorrelation processes within volume layer occur much faster than on the ground. The reason for this is that the scatterers in the canopy are less stable than ones on the ground. On the other hand, the temporal decorrelations of γ_{TV} and γ_{TG} are not only dependent on the wind-induced movement but also rely strongly on the rain-induced dielectric changes in volume and on the ground at temporal baselines on the order of days or

longer. Finally, the estimated temporal decorrelations γ_{TV} and γ_{TG} were converted to height errors and validated against the directly estimated height error from Pol-InSAR inversion. The obtained results are highly correlated on the order of 0.94 with an RMSE of 3.34%. This is a strong indication for the validity of the model used as well as for a successful estimation of γ_{TV} and γ_{TG} at temporal baselines on the order of days.

The behavior of temporal decorrelation on the order of minutes was strongly related to wind-induced movement and showed a rather random nature in forest due to the variability of wind pattern in space and time. For this time scale, changes in the electric properties of the canopy and the ground layer can be ignored. The wind speed of 2 m/s already reduces the performance of Pol-InSAR inversion dramatically by biasing the volume decorrelation over the test site. Therefore, the wind speed during the acquisition is the most critical parameter for the amount of temporal decorrelation for short repeat-pass time.

REFERENCES

[1] S. R. Cloude and K. P. Papathanassiou, "Polarimetric SAR interferometry," *IEEE Trans. Geosci. Remote Sens.*, vol. 36, no. 5, pp. 1551–1565, Sep. 1998.

[2] K. P. Papathanassiou and S. R. Cloude, "Single baseline polarimetric SAR interferometry," *IEEE Trans. Geosci. Remote Sens.*, vol. 39, no. 11, pp. 2352–2363, Nov. 2001.

[3] R. N. Treuhaft, S. N. Madsen, M. Moghaddam, and J. J. van Zyl, "Vegetation characteristics and underlying topography from interferometric radar," *Radio Sci.*, vol. 31, no. 6, pp. 1449–1495, 1996.

[4] S. R. Cloude and K. P. Papathanassiou, "Three-stage inversion process for polarimetric SAR interferometry," in *IEE Proc.—Radar Sonar Nav.*, Jun. 2003, vol. 150, no. 3, pp. 125–134.

[5] I. Hajnsek, F. Kugler, S.-K. Lee, and K. P. Papathanassiou, "Tropical-forest-parameter estimation by means of Pol-InSAR: The INDREX II campaign," *IEEE Trans. Geosci. Remote Sens.*, vol. 47, no. 2, pp. 481–493, Feb. 2009.

[6] R. Bamler and P. Hartl, "Synthetic aperture radar interferometry," *Inversion Probl.*, vol. 14, no. 4, pp. R1–R54, Aug. 1998.

[7] H. Zebker and J. Villasenor, "Decorrelation in interferometric radar echoes," *IEEE Trans. Geosci. Remote Sens.*, vol. 45, no. 10, pp. 950–959, Sep. 1992.

[8] F. Rocca, "Modeling interferogram stacks," *IEEE Trans. Geosci. Remote Sens.*, vol. 30, no. 5, pp. 3289–3299, Oct. 2007.

[9] K. P. Papathanassiou and S. R. Cloude, "The effect of temporal decorrelation on the inversion of forest parameters from Pol-InSAR data," presented at the IEEE IGARSS, Toulouse, France, 2003.

[10] I. Hajnsek, K. P. Papathanassiou, and S. R. Cloude, "Removal of additive noise in polarimetric eigenvalue processing," presented at the IEEE IGARSS, Sydney, Australia, 2001.

[11] R. Horn, "The DLR airborne SAR project E-SAR," presented at the IEEE IGRASS, Lincoln, NE, USA, May 1996.

[12] S. K. Lee, F. Kugler, K. P. Papathanassiou, and I. Hajnsek, "Multi-baseline polarimetric SAR interferometry forest height inversion approaches," presented at the POLinSAR, ESA-ESRIN, Frascati, Italy, Jan. 2011.

[13] Agrarmeteorologische Stationen [Online]. Available: http://www.lfl.bayern.de/agm/start.php

[14] T. Mette, "Forest biomass estimation from polarimetric and interferometry," Ph.D. dissertation, Technischen Universtät München, München, Germany, 2007.

[15] M. Lavalle, M. Simard, and S. Hensly, "A temporal decorrelation model for polarimetric radar interferometers," *IEEE Trans. Geosci. Remote Sens.*, vol. 50, no. 7, pp. 2880–2888, Jul. 2012.

[16] M. Neumann, L. Ferro-Famil, and A. Reigber, "Estimation of forest structure, ground, and canopy layer characteristics from multibaseline polarimetric interferometric SAR data," *IEEE Trans. Geosci. Remote Sens.*, vol. 48, no. 3, pp. 1086–1104, Mar. 2010.

[17] H. Kramer and A. Akca, *Leitfaden zur Waldmesslehre*. Frankfurt: Sauerländer, 1995, p. 145.

Seung-Kuk Lee received the B.S. and M.S. degrees from the Yonsei University, Yonsei, Korea, in 2000 and 2005, respectively, and the Dr. degree from ETH Zurich, Zurich, Switzerland, in 2012.

In 2007, he started working at German Aerospace Center (DLR), Wessling, Germany, as a Ph.D. student. He is currently working as a Research Scientist in Polarimetric SAR Interferometry research group at DLR. His main interests are 3-D forest parameter estimation using Pol-InSAR techniques, and quantification of temporal decorrelation effects for Pol-InSAR forest applications.

Florian Kugler was born in Bavaria, Germany, in 1974. He received a Diploma degree (Dipl.Ing.silv.) in forestry science from the Technische Universität München, Freising, Germany, in 2004. Since October 2004, he has been working toward the Ph.D. degree at the German Aerospace Center (DLR).

Since October 2008, he has been a Research Scientist at DLR. His research focuses on remote sensing on forests using polarimetric SAR interferometry.

Konstantinos Panagiotis Papathanassiou (M'02–SM'03) received the Dipl.Ing. degree (Hons.) and the Ph.D. degree (Hons.) from the Technical University of Graz, Austria, in 1994 and 1999, respectively.

From 1992 to 1994, he was with the Institute for Digital Image Processing (DIBAG) of Joanneum Research, Graz, Austria. Between 1995 and 1999, he worked at the Microwaves and Radar Institute (HR) of the German Aerospace Center (DLR), Oberpfaffenhofen, Germany. From 1999 to 2000, he was an EU Postdoctoral Fellow with Applied Electromagnetics (AEL) in St. Andrews, Scotland. Since October 2000, he has been with the Microwaves and Radar Institute (HR) of the German Aerospace Center (DLR), where he is a Senior Scientist leading the Information Retrieval research group. He has more than 100 publications in international journals, conferences and workshops. His main research interests are in polarimetric and interferometric processing and calibration techniques, polarimetric SAR interferometry, and the quantitative parameter estimation from SAR data, as well as in SAR mission design and SAR mission performance analysis.

Dr. Papthanassion was the recipient of the IEEE GRSS IGARSS Symposium Prize Paper Award in 1998, the Best Paper Award of the European SAR Conference (EUSAR) in 2002, and the DLR Science Award in 2002. In 2011, he was awarded with the DLR's Senior Scientist Award.

Irena Hajnsek (A'01–M'06–SM'09) received the Dipl. degree (Hons.) from the Free University of Berlin, Berlin, Germany, in 1996, and the Ph.D. degree (Hons.) from the Friedrich Schiller University of Jena, Jena, Germany, in 2001.

From 1996 to 1999, she was with the Microwaves and Radar Institute (DLR-HF) of the German Aerospace Center (DLR), in Oberpfaffenhofen, Germany. From 1999 to 2000 she was with the Institut d'Electronique et de Télécommunications de Rennes at the University of Rennes 1, France for 10 months, and with the Applied Electromagnetics (AEL) in St. Andrews, Scotland, four months in the frame of the EC-TMR Radar Polarimetry Network. In 2005, she was a guest Scientist at the University of Adelaide, Adelaide, South Australia, for six weeks. She is the Science Coordinator of the German satellite mission TanDEM-X. Her main research interests are in electromagnetic propagation and scattering theory, radar polarimetry, SAR and interferometric SAR data processing techniques, environmental parameter modelling and estimation.